ANALYSIS OF HYDROACOUSTIC SIGNALS IN THE INDIAN OCEAN

M. Tolstoy and D.R. Bohnenstiehl

Lamont-Doherty Earth Observatory, Columbia University

ABSTRACT

Hydroacoustic processing software developed over the past decade by National Oceanographic and Atmospheric Administration Pacific Marine Environmental Laboratory (NOAA/PMEL) has been modified to process CSS 3.0 format data from hydroacoustic stations within the Indian Ocean. This allows for the simultaneous inspection of multiple hydrophone channels, displaying trace amplitudes and spectrograms. When the hydroacoustic station at Crozet (H04) comes online in February 2003, this software package will allow events within the Indian Ocean Basin to be rapidly located solely on the basis of hydroacoustic arrivals, using a non-linear least squares algorithm that minimizes the differences between recorded and predicted T-wave arrives. Previous work in other ocean basins suggests that this approach will improve significantly our detection capability and location accuracy for Indian Ocean earthquakes. Given the final configuration of the Indian Ocean Hydroacoustic Network (stations H04, H08, H01), point-source simulations suggest location accuracy of ~2 km (68% level) within much of the array, assuming a random arrival error with normal distribution and standard deviation of 0.75 s for all channels. However, errors within the ocean sound velocity model and the width of the T-wave source region will decrease the accuracy of locations within the basin.

Commonly detected signals at the existing Diego Garcia (H08) and Cape Leeuwin (H01) hydrophones include a range of seismic phases (most commonly T, P and S), marine mammal vocalizations, ice-sheet movements, airguns and shipping noise, as well as other presently unidentified sounds that may be anthropogenic or natural in origin. Initial estimates of station noise levels indicate that Diego Garcia North is the quietest station, followed by Diego Garcia South and then Cape Leeuwin. When a full year's data have been analyzed, a catalog of annual noise variations will be merged with seismic and T-wave derived earthquake catalogs to examine the impact of noise on the hydrophones array's detection and location capabilities.

The natural seismicity within the ocean basin is used to map out areas of topographic blockage. The expected arrival time at individual hydrophones is calculated from Reviewed Event Bulletin (REB) events and each hydrophone is inspected for detectable T-waves. Based on the presence or absence of signals, regions of topographic blockage are mapped for the H01 and H08 hydrophones. Preliminary analysis of 2002 data indicates that >3.0 m_b events within the deep basin should be detectable on at least one hydrophone triad, given the final configuration of the network.

The incorporation of CSS 3.0 format data into the NOAA/PMEL processing suite improves synergy between hydroacoustic and seismic datasets. In the future, T-wave arrivals at island atoll stations (such as COCO, Keeling Island) could be used jointly with the hydrophone stations to locate events within an ocean sound velocity model.

OBJECTIVES

Hydroacoustic monitoring is a critical component of the Comprehensive Nuclear-Test-Ban Treaty (CTBT). It ensures that nuclear tests conducted in the ocean, or in the lower atmosphere directly above the ocean, do not go undetected. As such, it is essential that sub-oceanic earthquakes and other natural acoustic sources can be identified and subsequently ruled out as explosions. This requires a full characterization of the geological, biological and man-made noises generated within an ocean basin on a day-to-day basis. Characterizing the source and location of various signals provides an important framework by which to further improve our understanding of hydroacoustic wave propagation. Moreover, as the hydroacoustic network expands into new areas of geologic and anthropogenic complexity, prioritizing such work ensures the timely and efficient use of the network as a monitoring tool.

Given the limited number of hydroacoustic stations within the present International Monitoring System (IMS) that report to the International Data Centre (IDC), we also must assess the ability of land-based stations alone, or in conjunction with a limited number of hydrophones, to accurately detect and locate events within the oceans.

The research presented here represents a preliminary characterization and quantification of Indian Ocean acoustic sources, using existing IMS hydroacoustic stations (Figure 1). The routine location of events using hydroacoustic sensors alone will begin once the Crozet hydroacoustic station comes on line. Existing techniques for locating events using topographic reflections are too labor intensive to be used for all the many thousands of events occurring in the Indian Ocean basin each year. As part of this research we have adapted existing academic hydroacoustic analysis software to incorporate both hydroacoustic and seismic data from the IMS. This software will allow rapid location of small events when the Indian Ocean network is completed and currently provides an efficient platform for event characterization and quantification. This includes not only identifying the source origin and signal strength but also providing station specific topographic blockage and background noise information.
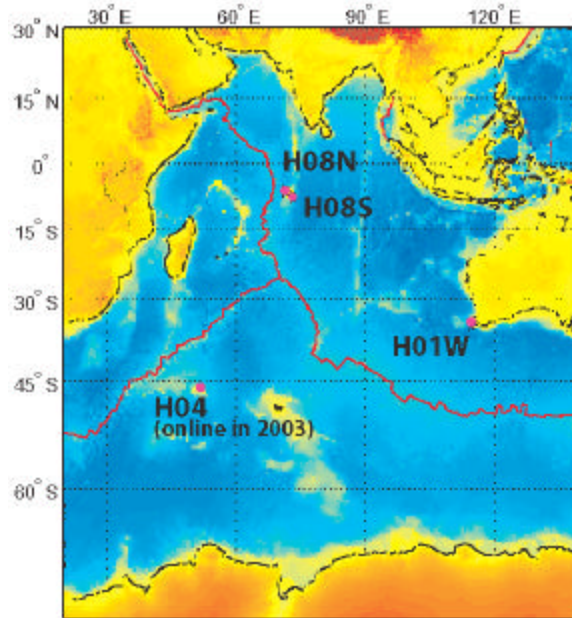

Figure 1. Location of IMS hydroacoustic stations in the Indian Ocean. Diego Garcia North & South (HO8N & HO8S) and Cape Leeuwin (HO1W) are currently operational. Crozet (H04) is expected to come on-line in February 2003. At each station there is a three-hydrophone array, or triad, with an instrument separation of ~2 km.

RESEARCH ACCOMPLISHED

Software

We have adapted the hydroacoustic analysis software developed at NOAA-PMEL (Fox et al., 2001) for use in the Indian Ocean. This work included the development of an Indian Ocean sound speed model (based on the Generalized Digital Environmental Model (GDEM) developed by the US Naval Oceanographic Office) and writing of conversion code to allow the CSS format data to be read directly into the software. The software allows data from different stations to be visually inspected, side by side, (Figure 2) and for events to be picked and located.

Based on the final configuration of the Indian Ocean Hydroacoustic Network (when the Crozet stations are operational), point-source simulations are used to predict the expected location errors. Figure 3 shows expected location error for events observed on at least three of the hydroacoustic stations (H-08S, H-01 & H04). The event location and magnitude is calculated based on an iterative, non-linear least squares method developed at NOAA-PMEL in which the sound is propagated through the ocean medium as represented by digital sound speed, in this case the GDEM model. A preliminary location and source time is used to predict arrival times at each sensor. The predicted time is compared to recorded arrival times, and the differences iteratively minimized using a Gradient-Expansion (Marquardt) algorithm, a least-squares method. Following the determination of the position and source time, statistics are calculated and a simple spherical and cylindrical propagation equation is used to estimate propagation loss for each path. This factor is applied to the peak recorded acoustic energy for each sensor and multiple independent estimates of the source strength calculated. The mean and variance of this estimate is saved (Fox *et al.* 2001). Based on the final configuration of the Indian Ocean Hydroacoustic Network (when the Crozet hydrophones are operational), point-source simulations are used to predict the expected location errors. Figure 3 shows expected location errors in kilometers for point-source events observed on at least three of the hydroacoustic stations (H-08S, H-01 & H04).
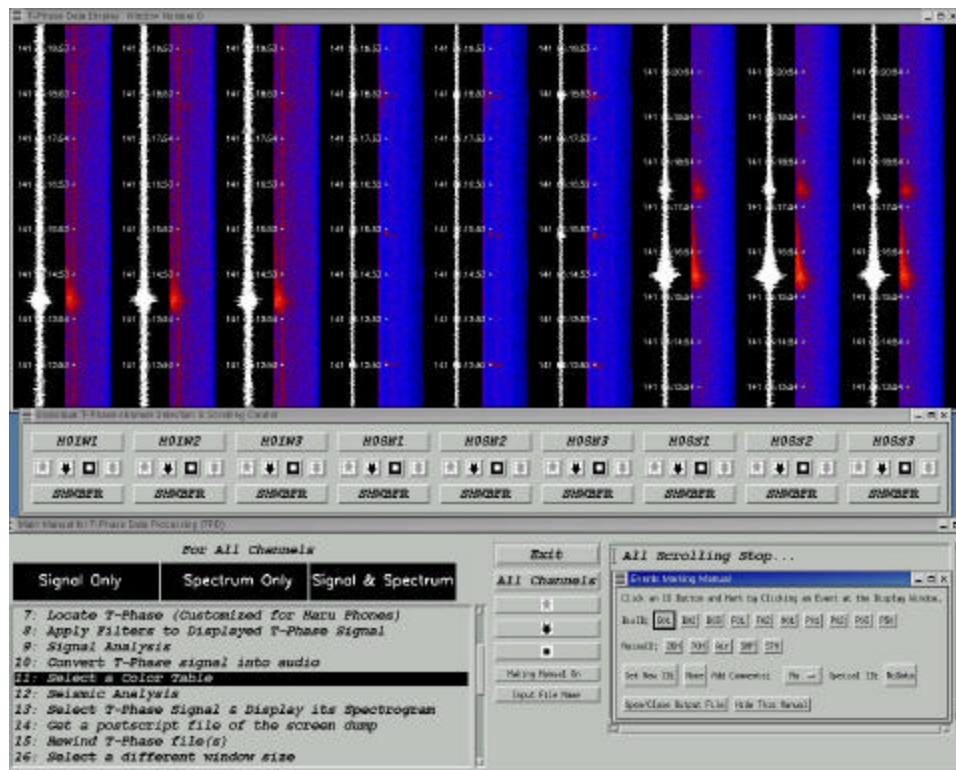

Figure 2. Example of software interface with data being simultaneously scrolled at all three hydroacoustic sites. Time increases on vertical axis, with trace amplitudes and 0-125 Hz spectrograms displayed.
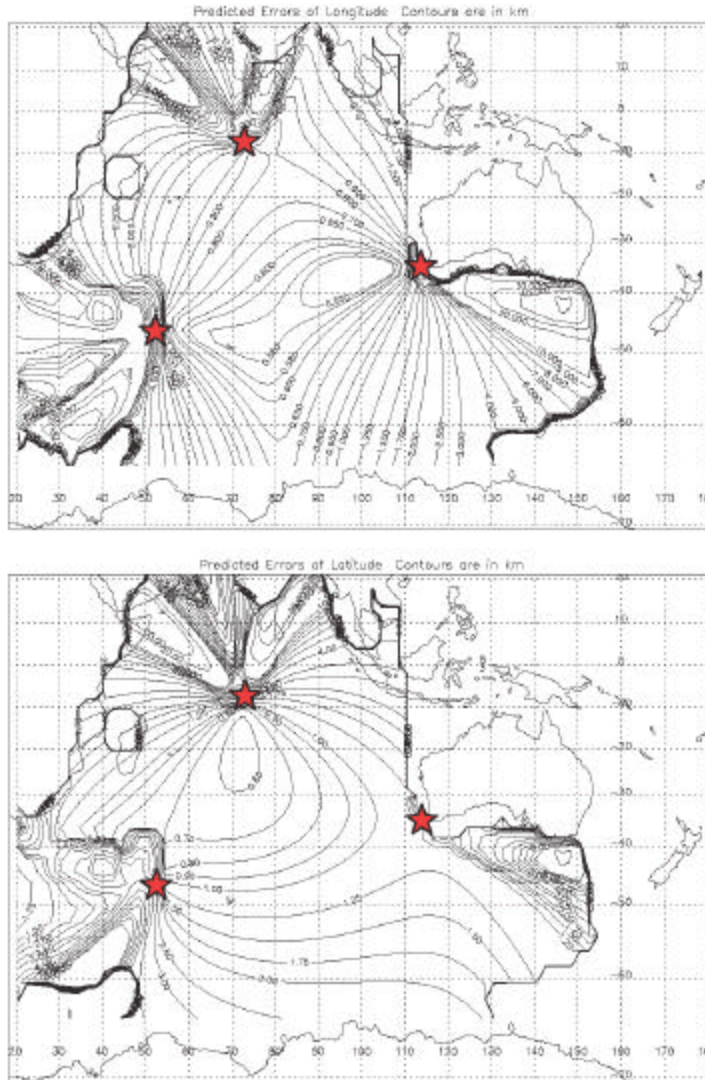
Figure 3. Predicted point-source location errors using an Indian Ocean sound speed model for the anticipated hydrophone configuration in February 2003 (see Figure 1). Location error estimates in latitude and longitude represent the 1σ (68%) confidence level and are given in kilometers. The error field was generated from Monte Carlo simulations of point sources and assumes arrival picks from six hydrophones (two at each triad, red stars). For each simulation the point-source location is prescribed and a random error with normal distribution and 0.75-s standard derivation is added to each arrival. The standard deviation of the picking error is based on calibrations within the Pacific (Fox *et al.*, 2001). Location errors may be larger due to uncertainties in sound speeds along the path, which are not well known, and the width of the T-wave source region on the seafloor. However, similar to arrays in the Atlantic and Pacific Oceans, we expect to be able to calibrate the Indian Ocean array using known sources.

Synergy with land seismic data

The software development completed now allows data from land-based seismic stations to be scrolled simultaneously along side the hydroacoustic data (Figure 4). For stations near the coast, a simple time correction (to allow for the faster travel time of the crustal borne portion of the T-wave) would allow near shore stations to be used as additional T-wave monitoring sites, thus improving location accuracy.
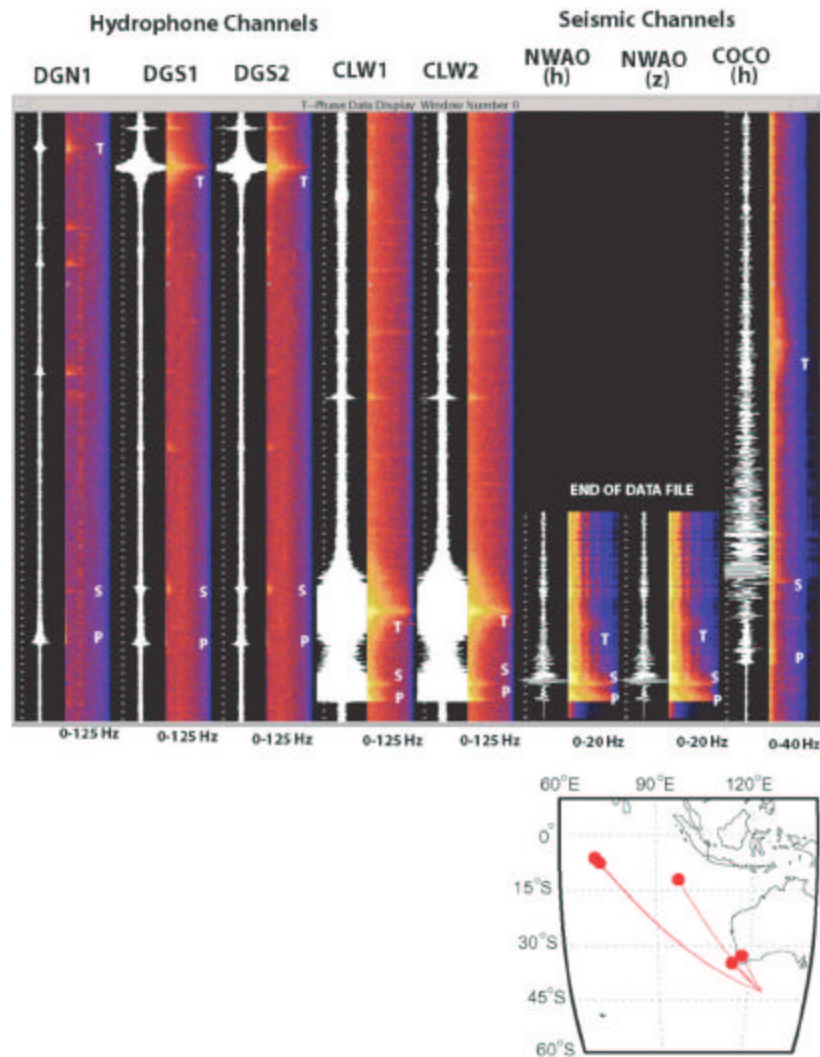
Figure 4. Example of arrivals from a large ocean basin event (7.1 Mw, JD 346, 2001) on hydrophones (HO8N, H08S & HO1W), and land seismic stations in southwestern Australia (NWAO) and Cocos/Keeling Island (COCO). Great circle paths are shown below. NWAO is ~200 km from the shelf where the T-wave would be converted into a crustal phase, so it is not ideal. However, the event was large enough that some T-wave related energy is still observed. Note it is about the same distance from the event as HOW1, and the P & S arrivals come in at the same time. The T-wave energy arrives earlier at NWAO, however, since it travels at faster crustal velocities for the last ~200 km of its path. The COCO station is located on a small island atoll, providing a short seismic path and excellent T-wave recording.

Event Characterization

Characterization of events is accomplished through visual inspection of the data, primarily in spectrogram form. Considerations in determining the event type include frequency content, duration, pattern through time, and relative amplitude if it is seen at both HO8 and HO1. While some signals are apparent in the waveform data, the spectrogram is much more informative, as seen in some of the examples below (Figure 5). Event characterization is important for a number of reasons. First, it is the initial step that must be taken before quantifying events and characterizing the 'typical' background signals in the Indian Ocean. Further, it will enable improved detection algorithms to be developed by establishing the amplitude and time/frequency range of various known signals.
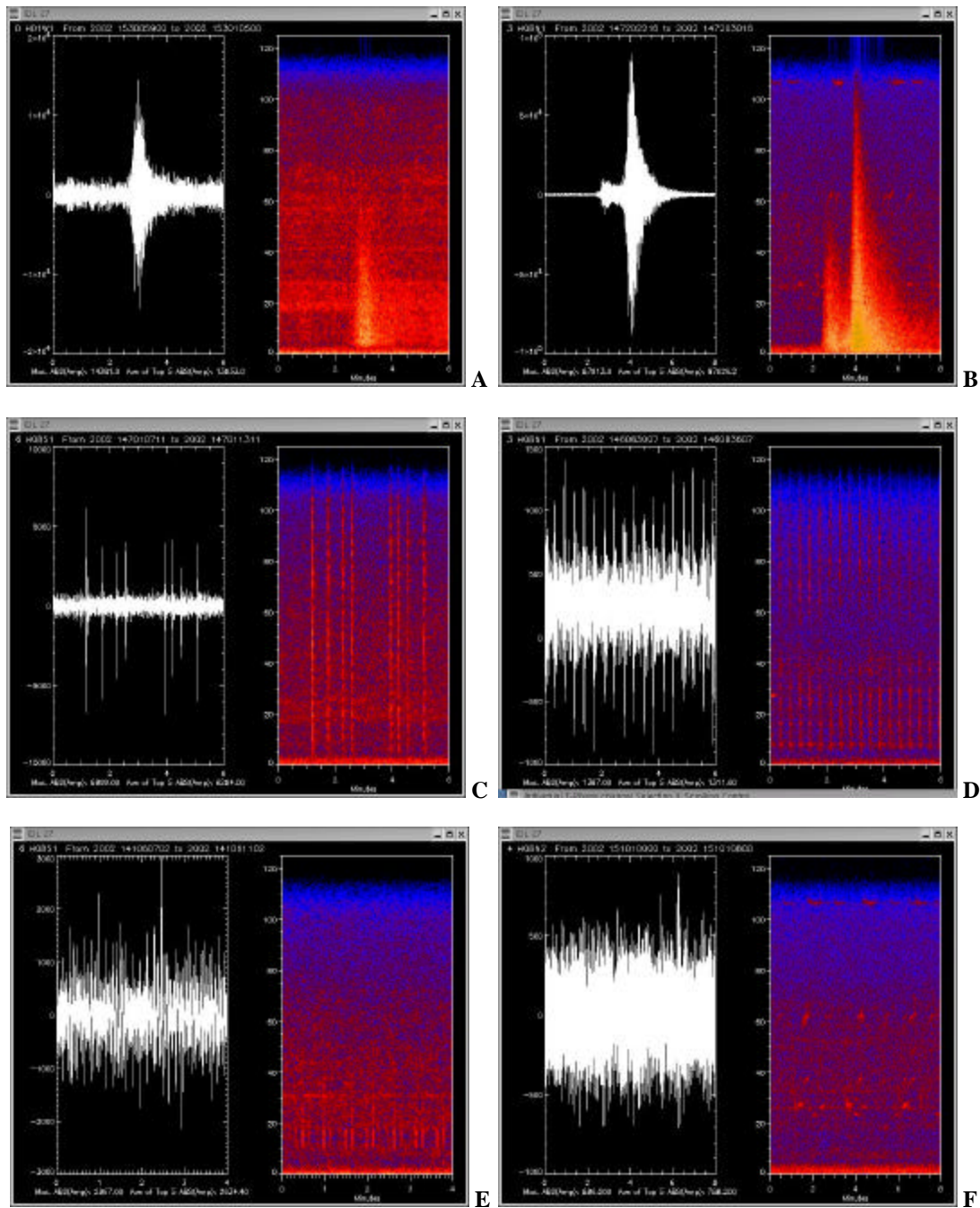
Figure 5: Examples of events observed regularly in the Indian Ocean. A) Typical T-wave arrival. B) P-wave arrival, followed by T-wave arrival. P-waves can be distinguished form T-waves by their more abrupt initiation. C) These 'spikes' look similar to airguns, but do not show the regular repeat intervals of airguns, and sometimes show up as individual spikes, without any indication of airgunning in the area before or after. These are of concern as possible explosive signals. D) Airgunning is frequently observed, but is easily distinguished from an explosion by its regular repeat interval (often 10 or 20 seconds). E) Fin Whale. F) Blue Whale.

G

H
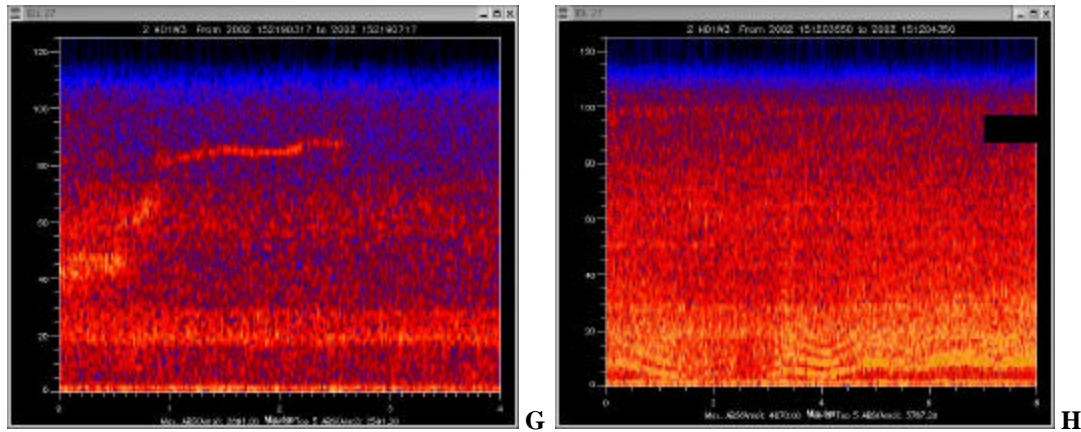
Figure 5. (continued) Examples of events observed regularly in the Indian Ocean. G) This high-frequency 'screech' may be biological in origin (perhaps a whale call). H) These low-frequency signals consist of monochromatic bands that evolve, or undulate, through time. They are similar in nature to T-phase signals associated with the movement of icebergs off the Antarctic shelf, as described by Talandier et al. (2002) from island stations in Polynesia.

A quantification of some of these signals for one week can be found in Table 1. Note final column on Table 1 is described as 'sharp signals'. These refer to events similar to what is seen in Figure 5C, where there is a sharp signal that cannot be associated with airgunning or other obvious causes, and therefore may be explosive in origin. The number of events detected at any given station is likely to vary from week to week (or day to day as shown) depending on levels of local and regional seismicity, and seasonal variations in anthropogenic (shipping, airgunning) and natural (mammal vocalizations, ice movement) background noise sources. Such variation may impact our ability to detect and locate other signals.

This table represents the number of times each feature was identified in the hydrophone data. The P- and T-wave arrivals were marked every time an event was seen. The air guns were marked every hour making 24 the greatest number of events allowed in one day. The whale calls were marked each hour every time a unique signal was seen (i.e. one hour may be marked twice if different whale species were observed within that hour). Many individual whale calls lasts for over an hour and were marked for each hour in which they appeared.

Table 1. Event quantification for week of May 26th – June 1st 2002.

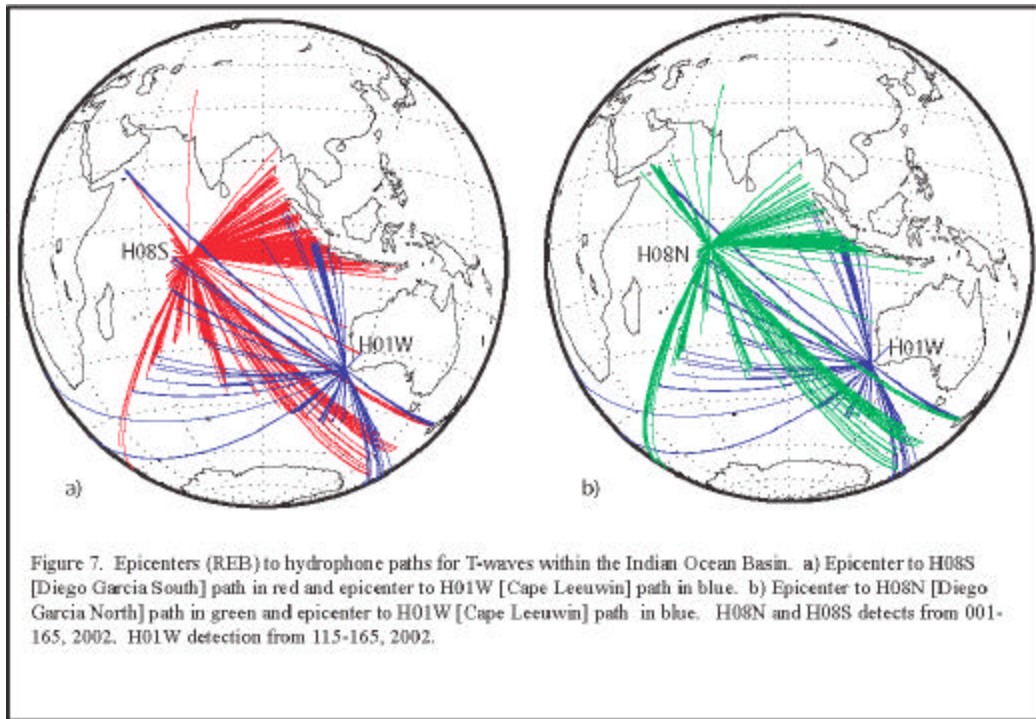| Day	T-Waves			P- and S-Waves			Air Guns (out of 24)			Whales			Sharp Signals		
	H01W	H08N	H08S	H01W	H08N	H08S	H01W	H08N	H08S	H01W	H08N	H08S	H01W	H08N	H08S
146	12	6	8	0	10	4	2	5	0	5	23	4	1	1	1
147	12	20	15	0	4	2	3	8	0	14	34	28	1	1	6
148	18	12	8	0	5	2	3	6	0	8	28	11	2	0	2
149	35	13	13	0	6	1	3	0	0	10	22	15	2	0	11
150	23	11	14	0	5	1	3	0	0	1	17	14	1	1	3
151	22	13	4	1	6	1	0	0	0	4	27	22	3	0	9
152	12	10	6	0	6	1	0	0	0	2	25	22	0	0	6
Total	135	85	68	1	42	12	14	19	0	44	176	116	10	3	38

Topographic Blockage
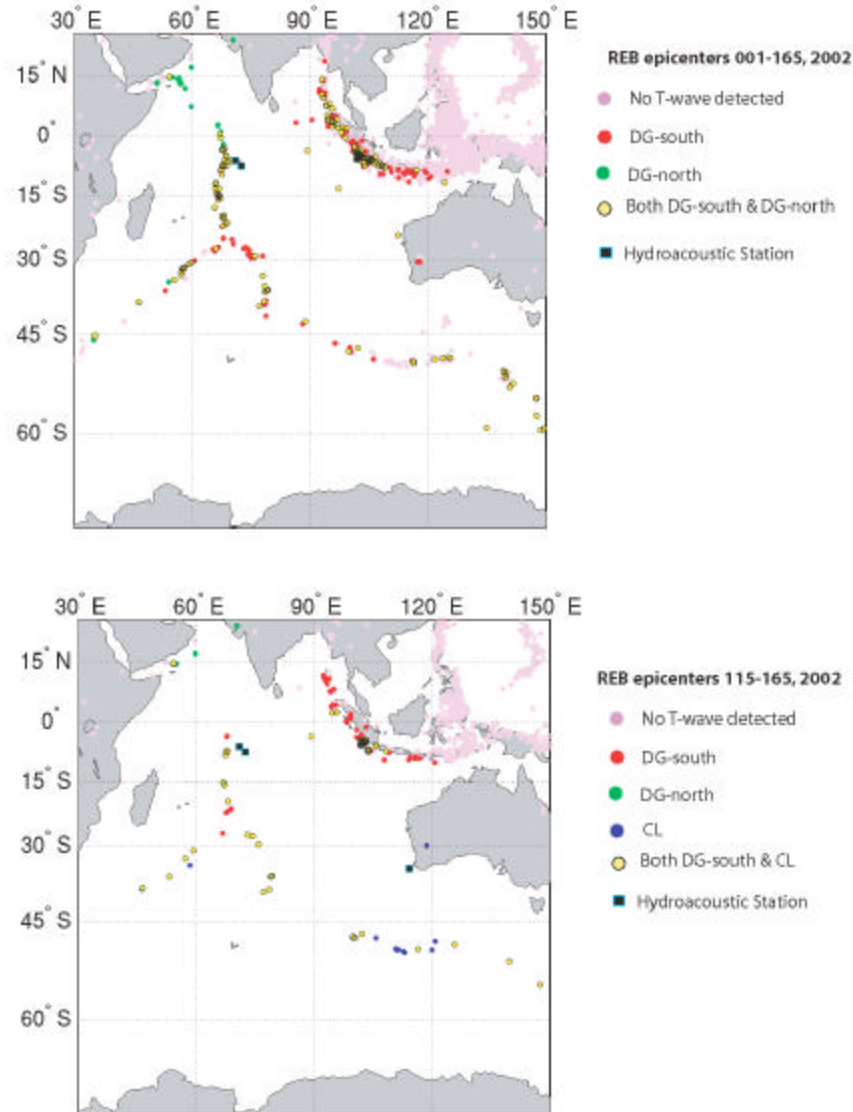
Figure 6. Locations of > 3.0 m$_b$ events listed in the REB and observed at the Diego Garcia and Cape Leeuwin hydroacoustic stations. Top figure shows events for Julian days 1-165, 2002, for Diego Garcia stations only. Bottom figure shows events for Julian days 115-165, 2002, (CL arrival data become available through the REB on day 115) as observed on all three stations. Note that some events were observed at DG-North, as well as DG-South and CL, but are covered by the yellow symbols.
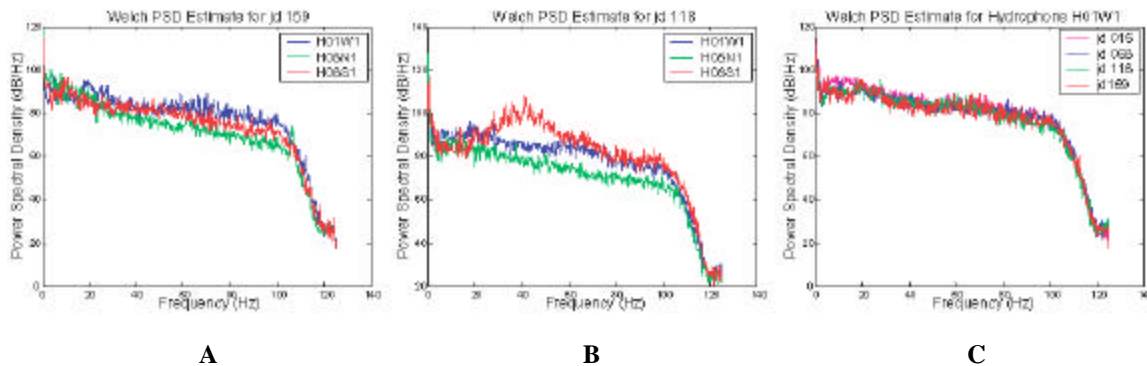
Predicted paths of topographic blockage can be modeled using seafloor bathymetry maps and station locations (e.g. Pulli and Upton, 2001); however, this is sometimes dependent on poorly known bathymetry and varies with event magnitude. Another approach is to examine the T-wave arrival records for known events, which were located using land station body wave arrivals (e.g. also Pulli and Upton, 2001). Below we present some initial results based on events observed in 2002. Figure 6 shows the events in the first 165 days of 2002 that were observed at Diego Garcia (HO8N & HO8S), as well as events that were observed at Cape Leeuwin (H01) and Diego Garcia from Julian days 115-165 (when Cape Leeuwin arrival data are available). These figures illustrate that there is reasonably good coverage to single stations within the Indian Ocean. Figure 7 indicates the raypaths for these hydroacoustically

detected events, and so provides a map of areas where complete blockage does not occur. However, there is also clear evidence that the magnitude of the event can impact degree of blockage. For example, in the top panel of Figure 5 there is a cluster of events at ~ 43S, 125E that are not observed at Diego Garcia South (HO8S). These events are aftershocks of a very large (Mw=7.1) earthquake in the same area in December 2001 that *was* observed at Diego Garcia South – (see Figure 4.). These much smaller magnitude events in early 2002 were not large enough to be detected above background noise at the H08, perhaps due in part to partial blockage associated with Broken Ridge (the elevated area running along ~32°S west of Cape Leeuwin).

Figure 7. Epicenters (REB) to hydrophone paths for T-waves within the Indian Ocean Basin. a) Epicenter to H08S [Diego Garcia South] path in red and epicenter to H01W [Cape Leeuwin] path in blue. b) Epicenter to H08N [Diego Garcia North] path in green and epicenter to H01W [Cape Leeuwin] path in blue. H08N and H08S detects from 001-165, 2002. H01W detection from 115-165, 2002.

Background Noise

| A | B | C |

Figure 8. Daily noise spectra for HO8N, HO8S and HO1W. A) Spectra for Julian Day 159, 2002, at all three sites. B) Spectra for Julian Day 118, 2002, at all three sites. Note the influence of a particularly loud ship in HO8S (red). C) Spectra for various days from January 15th through June 8th at HO1W.

The background noise at hydrophone sites is controlled by a number of factors including proximity to shore (wave noise), weather variations and shipping in the area. The level of background noise is a critical factor in the ability of a station to observe specific events. As background noise increases, the detection sensitivity of the station decreases accordingly. Many noise sources are seasonal; therefore, it is important to characterize the noise for the full annual

spectrum. Previous work at Diego Garcia (Hanson, 2001) has shown that Diego Garcia North is quieter than Diego Garcia South, and that both sites show a slight decrease (~3db) in noise level between January and July. Figure 8a illustrates that in general Diego Garcia North is quieter than Diego Garcia South, and that both are quieter than Cape Leeuwin. However, Figure 8b shows that this can vary on a daily basis when unusual noise sources are present. Figure 8c shows a snapshot of Cape Leeuwin daily noise profiles at various dates from January through May 2002. No clear seasonal variation is apparent, but since daily noise variations are susceptible to local events, a more detailed look at more days is required before drawing any conclusions. Eventually daily, weekly and monthly averages will be provided when a full year's data has been delivered and analyzed.

CONCLUSIONS AND RECOMMENDATIONS

We have adapted existing hydroacoustic processing software to read the CSS 3.0 format. This allows hydroacoustic data from the presently available H08 (Diego Garcia) and H01 (Cape Leeuwin) stations to be examined by an analyst in an efficient manner, viewing both amplitude traces and spectrograms. These modifications also will facilitate increased synergy between seismic (island or near shore stations) and hydroacoustic data sets.

As data from the H04 (Crozet) hydrophones become available, earthquake events will be located solely on the basis of T-wave arrivals. Previous work and limited ground truth in other ocean basins suggests this approach will improve significantly our ability to detect and locate moderate size earthquakes and other hydroacoustic signals.

Using the data presently available from H08 and H01, we have begun an effort to characterize and catalog sound sources within the Indian Ocean Basin. These include seismic phases, marine mammal vocalizations, airguns and possible ice-sheet movements. Initial noise estimates indicate that Diego Garcia South appears to be the quietest triad, followed by Diego Garcia North and then Cape Leeuwin.

Initial blockage results indicate good spatial coverage of much of the Indian Ocean by at least one hydrophone.

ACKNOWLEDGEMENTS

REFERENCES

Fox, C.G., H. Matsumoto, and T.-K. Lau (2001), Monitoring Pacific Ocean Seismicity from an Autonomous Hydrophone Array, *J. Geophys. Res.*, **106**, 4183-4206, 2001.

Pulli, J.J., and Z.M. Upton (2001), Hydroacoustic Blockage at Diego Garcia: Models and Observations, *Proceedings of the 23rd Seismic Research Review*, Vol. II, 45-54.

Hanson, J.A. (2001), Initial Analysis of Data from the New Diego Garcia Hydroacoustic Station, *Proceedings of the 23rd Seismic Research Review*, Vol. II, 12-22.

Talandier, J., P.-F. Piserchia and E.A. Okal (2002), Hydroacoustic signals detected in Polynesia from mega-iceberg drifting in the Ross Sea, Antarctica, *abstract, annual meeting SSA, Seismological Research Letters*, **73**, 217.